7

Application of Kalman Filter to Bad-Data Detection in Power System

Chien-Hung Huang, Kuang-Kong Shih,
Chien-Hsing Lee and Yaw-Juen Wang
Taiwan Power Company, National Formosa University of Science and Technology, National Cheng Kung University& National Yunlin University of Science and Technology Taiwan

1. Introduction

Bad-data detection in pre-estimation can help to improve state estimation [Teeuwsen & Erlich, 2006]. Since transient and abnormal conditions may occur in a power system, measurements may be polluted by bad data to cause estimated errors. Hence, it is necessary to accurately detect the bad data. To ensure the reliability of the measured data, a practical state estimator should have an ability to detect and identify the bad data as well as to eliminate their effects on the estimation [Zhang & Lo, 1991].

Generally, bad-date detection is important to guarantee the reliability of the measured data. If one or more errors occur in power system measurements, the states of the estimated system may be biased and the safety of power supply may be potentially dangerous. To avoid this situation, several bad-data detection and identification schemes have been presented. For example, WLS (weighted least squares) was proposed in 1989 [EI-Keib et al., 1989]. The weighted sum of squares of the measurement residuals was chosen as the objective function to be minimized. But, WLS-based state estimators were only developed by using a linearized measurement function [Huang & Lin, 2003] with complicated computations. Then, linear programming (LP) was proposed to improve the identification method [Peterson & Girgis, 1988]. However, the LP estimator may fail to reject the bad data and it can be attributed to the existence of leverage in the power system model [Ali Abur, 1990]. Thus, Ali Abur had proposed hypothesis testing identification (HTI) to extend the case of the LP estimator. Nevertheless, it had caused computational burdens with taking the special properties of the LP estimation equations into account. Huang [Huang & Lin, 2003] proposed a changeable weighting matrix to identify the bad data but it only can apply for static state estimations. Nevertheless, Zhang had proposed recursive measurement error estimation identification (RMEEI) for bad-data identification [Zhang et al., 1992]. State variables, residuals and their parameters can be updated after removing a measurement from the suspected data set to the remaining data set by using a set of linear recursive equations. With splitting the raw measurements into some parts, a set of residual equations used by the traditional methods can only apply to linear systems and it may result the operation of calculation burden and complexity because each part consists of some measurements [Zhang et al., 1992].

Source: Kalman Filter, Book edited by: Vedran Kordić,
ISBN 978-953-307-094-0, pp. 390, May 2010, INTECH, Croatia, downloaded from SCIYO.COM

Thus, an artificial neural network (ANN) technique was proposed to overcome this problem. Moreover, data projection technique [Souza, et al,. 1998] is proposed, the normalized innovations are used as input variables to construct ANN based on the Group Method of Data Handling (GMDH) for bad data identification. Pattern analysis techniques [Alves da Silva, et al., 1992] is developed which based on a probabilistic approach with implementing ANN to correct the bad data in critical measurements. The ANN can find a nonlinear function mapping between input and output through the trained weights; meanwhile, it can be considered as an estimator to filter abnormal variations from input not the output. This means noise or large variations can be eliminated or depressed if they occur at the ANN input. Furthermore, the ANN can process raw estimated measurements by the trained ANN to diagnose bad data with a threshold value [Salehfar & Zhao, 1995] or gap-statistic-algorithm [Teeuwsen & Erlich, 2006; Huang & Lin, 2004]. Its advantage is that most measured errors can be identified and responded quickly but the pre-requisite is under a well training to construct the nonlinear function between input and output. In literature [Teeuwsen & Erlich, 2006; Salehfar & Zhao, 1995; Huang & Lin, 2002], the back-propagation algorithm has usually been applied to train the ANN. However, it has several drawbacks as follows:

1. The complex quantities measured in a power system need to separate into two parts since the standard ANN only uses real numbers as variables. This increases the size of the neural model to result poor convergence behavior. Although Salehfar and Zhao [Salehfar & Zhao, 1995] had proposed a divided technique to solve this problem, it will increase the number of iterations in the learning stage. Thus, the divided technique is labor-intensive and inconvenient.
2. The nonlinear mapping function used in power system measurements is complex and cannot be implemented with the standard ANN. Thus, the filtering performance is degraded. This means the standard ANN may not be able to remove noise and abnormal variations well at the input.
3. The training method used in the standard ANN is based on the back-propagation algorithm. However, the back-propagation algorithm cannot validly keep immunity from noise on the training data. Thus, the nonlinear function will be affected by the training algorithm in bad mapping.
4. The learning rate is not sure to be suitably applied because of the heuristic choice. It may incur the problem of stability and suffer from much slower convergence if an improper learning rate is chosen. Moreover, the learning rate is usually adjusted at the training stage for different systems. This is inconvenient for applications.

To overcome those drawbacks, in this chapter we proposes an extended complex Kalman filter artificial neural network (ECKF-CANN). It can perform well on bad-data identification with fast computational speed in two stages. The first stage is the learning process. State variables consist of the weighting that can be learned using extended complex Kalman filter (ECKF) to achieve the purpose of adjusting the learning of artificial neural network (ANN) constantly. As the training has been finished, similarly, a polluted value with several times of the standard deviation of the measurements was added into the measurements. The second stage uses the complex ANN (CANN) with the trained weighting to estimate the measurements. The rule of bad-data decision is to minimize the square difference between the measured and estimated values.

2. Complex artificial neural network

This chapter uses the ECKF algorithm to train the weightings of the ANN since the ECKF can estimate continually to modify the weightings in order to reach the learning purpose of the ANN without the learning parameter at the learning stage. Then, the trained CANN can be used for bad data detection. Moreover, the proposed ECKF-CANN method can increase the magnitude of the squared errors to enhance the efficiencies of bad data detection as bad data have been occurred because the nonlinear mapping function of the CANN and the complex measurements are coordinated well and the ECKF has a pre-filtering characteristic. A framework of the proposed ECKF-CANN method is shown in Fig. 1. As seen in Fig. 1, this method uses two algorithms. One is the artificial neural network (ANN) with complex-type variables; the other is the extended complex Kalman filter (ECKF) to train the link weightings of the complex ANN (CANN).

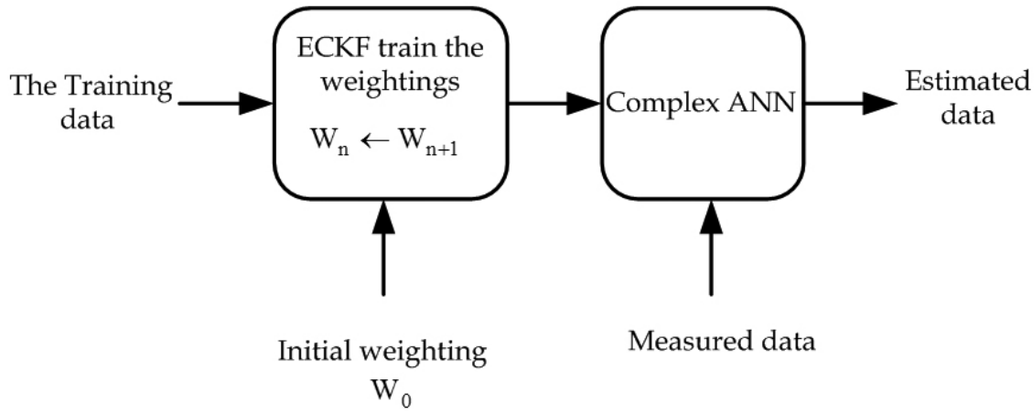

Fig. 1. Framework of the ECKF-CANN method.

The structure in the n^{th} neuron of the L layer is shown in Fig. 2. The input complex signal can be separated into real and imaginary parts. The output is a complex-type by operating with the activation function $f(\bullet)$ to suppress the varying range of the input signal. The relation of input and output of the neuron is written to be

$$O_n^L = f(S_n^L) = f(S_{n,R}^L) + jf(S_{n,I}^L) \tag{1}$$

Note that $O_{n,R}^L$ and $O_{n,I}^L$ as shown in Fig. 1 are the real and imaginary parts of the output neuron O_n^L, respectively.

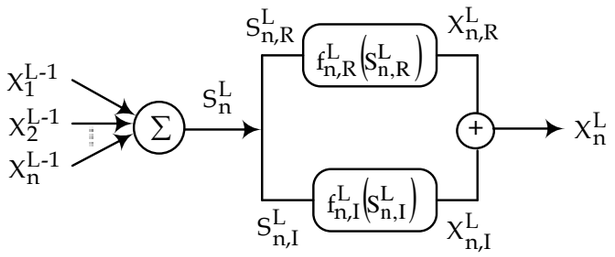

Fig. 2. Configuration of complex neurons.

Similarly, $S_{n,R}^{L}$ and $S_{n,I}^{L}$ are the real and imaginary parts of the input neuron $S_{n,}^{L}$, respectively. S_{n}^{L} is a linear combination of the output of the prior layer and is represented by the following equation.

$$S_n^L = S_{n,R}^L + jS_{n,I}^L = \sum_{m=1}^{n} O_n^{L-1} * W_{nm}^{L-1} \tag{2}$$

In (2), W_{nm}^{L-1} denoted the weighting of the prior layer is also a complex-type. Its operating structure is shown in Fig. 3 and the relation of the input data and the weighting is written to be

$$\begin{aligned} O * W &= (O_R + jO_I)(W_R + jW_I) \\ &= (O_R * W_R - O_I * W_I) + j(O_R * W_I + O_I * W_R) \end{aligned} \tag{3}$$

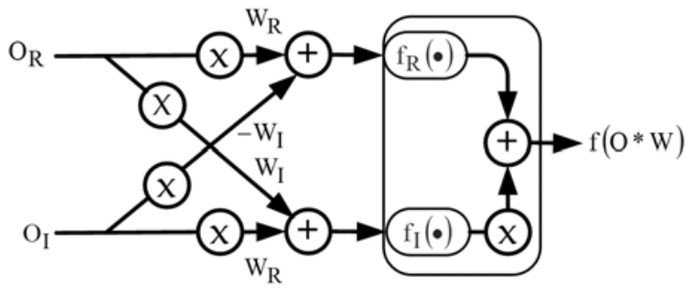

Fig. 3. Configuration of data resolution.

Substituting (3) into the activation function $f(\bullet)$, one can obtain

$$f(O * W) = f(O_R * W_R - O_I * W_I) + jf(O_R * W_I + O_R * W_I) \tag{4}$$

To satisfy the conditions of the activation function, a complex activation function is obtained by conforming to a special property which it is analytic and bounded everywhere in the complex plane [Taehwan Kim & Adali, 2000]. This paper selects the function of $\tanh(z)$ as an activation function, where z is a complex value.

3. Extended complex Kalman filter

The ECKF-CANN method is proposed to use the innovation vector to minimize the difference between input and output. The unknown link weighting w of the ECKF-CANN method [Deergha Rao, 1996; Deergha Rao et al., 2000; Taehwan Kim & Adali, 2000] from the first layer to the M layer can be considered as state variables of the ECKF for estimations as below:

$$w = [(w^1)^T, (w^2)^T, (w^3)^T, ..., (w^{M-1})^T]^T, (L \times 1) \tag{5}$$

where superscript T is the matrix transpose operation, L indicates the total number of the sum of link weighting. If N_n is the number of the neuron in the n layer, the link weighting at i^{th} node of the n layer w_i^n is written to be

$$w_i^n = [w_{i,1}^n, w_{i,2}^n, w_{i,3}^n, ..., w_{i,N_n}^n]^T, (N_n \times 1) \tag{6}$$

The link weighting w^n of the n layer is expressed to be

$$w^n = [(w_1^n)^T, (w_2^n)^T, (w_3^n)^T, ..., (w_{N_{n+1}-1}^n)^T]^T,$$

$$(N_n(N_{n+1} - 1) \times 1) \tag{7}$$

and the total number of the link weighting of the CANN is given to be

$$L = \sum_{n=1}^{M-1} N_n (N_{n+1} - 1). \tag{8}$$

Assuming the output $O^n(t)$ of the nodes at n^{th} layer can written to be

$$O^n(t) = [O_1^n(t), O_2^n(t), ..., O_{N_n}^n(t)]^T, (N_n \times 1) \tag{9}$$

and the desired output $d(t)$ is given to be

$$d(t) = [d_1(t), ..., d_{N_M}(t)]^T, (N_M \times 1) \tag{10}$$

As a result, the model of multilayered neural network can then be expressed by nonlinear equations as below:

$$w(t+1) = w(t) \tag{11}$$

$$d(t) = O^M(t) + v(t) \tag{12}$$

where $O^M(t)$ is the output layer of the CANN at an instant time t, M is the output of the last layer, v(t) is a random noise with covariance $R_v(t)$. Thus, the learning algorithm of the ECKF-CANN is summarized to be

$$\hat{w}(t) = \hat{w}(t-1) + K(t)[d(t) - \hat{O}^M(t)], (L \times 1) \tag{13}$$

$$K(t) = P(t-1)H(t)^H[H(t)P(t-1)H(t)^H + R_v(t)]^{-1},$$

$$(L \times N_M) \tag{14}$$

$$P(t) = P(t-1) - K(t)H(t)P(t-1), (L \times L) \tag{15}$$

where K(t) is the Kalman gain, H(t) is the measurement matrix, $H(t)^H$ is the Hermitian matrix of H(t) called the Jacobian matrix, $\hat{w}$ is the estimated value of w, and P(t) means the expectation values of the residual of the $\hat{w}(t)$ and $\hat{w}(t-1)$. One can further write the P(t) and H(t) to be as below:

$$P(t) = E\{(\hat{w}(t) - \hat{w}(t-1))(\hat{w}(t) - \hat{w}(t-1))^H\} \tag{16}$$

$$H(t) = \left(\frac{\partial O^M(t)}{\partial w}\right)_{w=\hat{w}(t-1)}$$

$$= \frac{\partial (O_R^M(t) + jO_I^M(t))}{\partial (w_R(t) + jw_I(t))}\Big|_{w=\hat{w}(t-1)}$$

$$= \left(\frac{\partial (O_R^M(t) + jO_I^M(t))}{\partial (w_R(t) + jw_R(t))}\right)_{w=\hat{w}(t-1)} + \left(\frac{\partial (O_R^M(t) + jO_I^M(t))}{\partial (w_I(t) + jw_I(t))}\right)_{w=\hat{w}(t-1)}$$

$$= [H_1^1(t), \ldots, H_{N_2-1}^1(t), H_1^2(t), \ldots H_{N_3-1}^2(t), \ldots, H_1^{M-1}(t), \ldots H_{N_{M-1}}^{M-1}(t)],$$

$$(N_M \times L) \tag{17}$$

and

$$H_i^n(t) = \left(\frac{\partial O^M(t)}{\partial w_i^n}\right)_{w=\hat{w}(t-1)}$$

$$= \left(\frac{\partial O_R^M(t)}{\partial w_{iR}^n}\right)_{w=\hat{w}(t-1)} + j\left(\frac{\partial O_I^M(t)}{\partial w_{iR}^n}\right)_{w=\hat{w}(t-1)}$$

$$+ \left(\frac{\partial O_R^M(t)}{\partial w_{iI}^n}\right)_{w=\hat{w}(t-1)} + j\left(\frac{\partial O_I^M(t)}{\partial w_{iI}^n}\right)_{w=\hat{w}(t-1)}, \; N_M \times N_n \tag{18}$$

$$H_i^n(t) = \Delta_{iRR}^n(t)|_{w=\hat{w}(t-1)} \hat{O}_R^n(t)^T + j\Delta_{iIR}^n(t)|_{w=\hat{w}(t-1)} \hat{O}_I^n(t)^T$$
$$+ \Delta_{iRI}^n(t)|_{w=\hat{w}(t-1)} \hat{O}_R^n(t)^T + j\Delta_{iII}^n(t)|_{w=\hat{w}(t-1)} \hat{O}_I^n(t)^T$$

$$= H_{iR}^n(t) + H_{iI}^n(t) \tag{19}$$

where

$$H_{iR}^n = \hat{\Delta}_{iRR}^n(t)|_{w=\hat{w}(t-1)} \hat{O}_R^n(t)^T + \hat{\Delta}_{iRI}^n(t)|_{w=\hat{w}(t-1)} \hat{O}_R^n(t)^T \tag{20}$$

$$H_{iI}^n = j\hat{\Delta}_{iIR}^n(t)|_{w=\hat{w}(t-1)} \hat{O}_I^n(t)^T + j\hat{\Delta}_{iII}^n(t)|_{w=\hat{w}(t-1)} \hat{O}_I^n(t)^T \tag{21}$$

$$\Delta_{iRR}^n(t) = (1 - (\hat{O}_{iR}^{n+1}(t))^2) \sum_{l=1}^{N_{n+2}-1} \hat{w}_{l,iR}^{n+1}(t-1) \hat{\Delta}_{lRR}^{n+1}(t) \tag{22}$$

$$\Delta_{iIR}^n(t) = (1 - (\hat{O}_{iI}^{n+1}(t))^2) \sum_{l=1}^{N_{n+2}-1} \hat{w}_{l,iI}^{n+1}(t-1) \hat{\Delta}_{lIR}^{n+1}(t) \tag{23}$$

$$\Delta_{iRI}^{n}(t) = (1-(\hat{O}_{iR}^{n+1}(t))^2)\sum_{l=1}^{N_{n+2}-1}\hat{w}_{l,iR}^{n+1}(t-1)\hat{\Delta}_{lRI}^{n+1}(t) \tag{24}$$

$$\Delta_{iII}^{n}(t) = (1-(\hat{O}_{iI}^{n+1}(t))^2)\sum_{l=1}^{N_{n+2}-1}\hat{w}_{l,iI}^{n+1}(t-1)\hat{\Delta}_{lII}^{n+1}(t) \tag{25}$$

Note that the noise of the training data can be depressed since the ECKF used to train the weightings of the CANN does not consider the learning rate with heuristics.

4. Bad data detection

For bad-data detection, complex-type data obtained from power flow calculations are used in this chapter. The data learned by the ECKF will be used to train the variety of the weightings and the architecture of Complex ANN filter is applied to estimate the polluted measurements.

Since the difference between the measured value X_i and the estimated value O_i at a particular measurement point is larger than a pre-specified detection threshold in the ECKF-CANN, the decision rule based on CANN is given by

$$(X_i - O_i)^2 > r_i^2,\ i = 1,\ldots,n \tag{26}$$

where the parameters i and r represent the measurement index and the threshold, respectively. An appropriate threshold is important for bad-data detection. Many trials have to be made in order to determine the best value. Generally, the square of 10 times standard deviation is chosen for each measurement index [Salehfar & Zhao, 1995]. Bad data can be flagged as the square of the residual between the measured and estimated values is larger than the corresponding threshold. Thus, the bad data can be detected. The procedure of bad-data detection is described as follows:

Step 1. Inputting normal measurement from a telemeter instrument at a control point such as voltages or power flows in a power system.

Step 2. Performing the learning phase of ECKF to estimate the link weighting.

$$S_n^{(L)} = \sum_{m=0}^{N_{L-1}} W_{nm}^{(L)} O_m^{(L-1)} \tag{27}$$

Step 3. Completing the learning as the residual is smaller than the accepted range during constant training of ECKF by the past historical data.

$$E = \sum_{n=1}^{N}((D_{nR} - O_{nR}) + (D_{nI} - O_{nI}))^2 \tag{28}$$

where D_{nR} and D_{nI} are the real and imaginary parts of the designed value, respectively. O_{nR} and O_{nI} are also the real and imaginary parts of the output of ECKF, respectively.

Step 4. Inputting the polluted measurement and executing the CANN algorithm.

Step 5. Determining bad data by squaring the difference between the estimated and measured values with the decision rule as shown in (26).

Step 6. Using the estimator to directly estimate with no bad-data existing. If bad data have occurred, the original measured value can be replaced by the estimated value and state estimation can be executed again.

The whole process of estimations as mentioned above may continue until the measurement index is beyond the time point obtained from the raw measurement.

5. Simulation

Two test systems including a 6-bus and the IEEE 30-bus power systems are used in this study. ANN configurations include input, hidden and output layers. The 6-bus system as shown in Fig. 4 consists of 6-bus voltage magnitude $|V_i|$, 3 pairs of active and reactive generations, 3 pairs of active and reactive loads Pi, Qi, and 22 pairs of active and reactive line flows Pi-j, Pj-i, Qi-j and Qj-i. Total of 62 data are measured in this system. Since the active and reactive power flows can be represented with a complex-type, the total measured data is then reduced to 34. As for the 30-buses system, it consists of 24 load buses, 5 generator buses and 1 reference (swing) bus as shown in Fig. 5. As a result, total of 142 data are needed to measure with the complex-type representation.

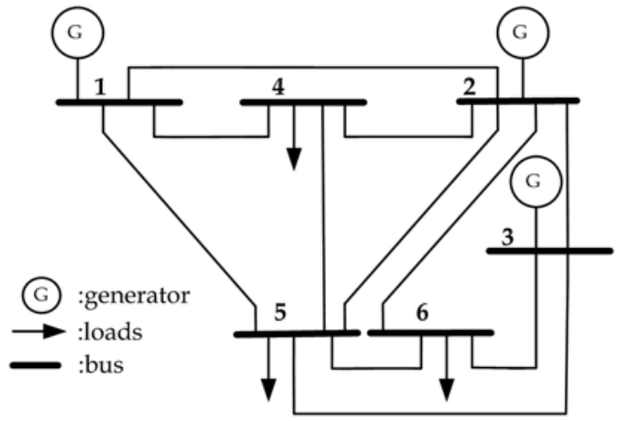

Fig. 4. Measurement configuration of 6-bus system.

Three methods will be used to detect the bad data, including ECKF-CANN, real back-propagation artificial neural network (RBP-ANN) and complex back-propagation artificial neural network (CBP-ANN). Moreover, abilities on convergences and noises rejection of the three methods are performed to assess their efficiency on bad-data detection. Comparison of the convergent behavior for detecting the 6-bus system using the three methods is shown in Fig. 6. As seen from Fig. 6, the squared error is 0.60726 at the 2nd number using the ECKF-CANN. However, the squared errors reach 0.94414 and 0.93272 at the 70th and 40th training number for the RBP-ANN and CBP-ANN, respectively.

To avoid interfering bad-data detection, the ability of noises injection is tested by applying above three methods and the results are shown in Fig. 7. As seen from Fig. 7 the squared error of the RBP-ANN reaches 0.45 at the noise of 18 dB. However, the squared errors of the CBP-ANN and ECKF-CANN reach only 0.0014461 and 0.00016034 at the noise of 20dB, respectively. Thus, performance on noise injection using the ECKF-CANN is the best among the three methods.

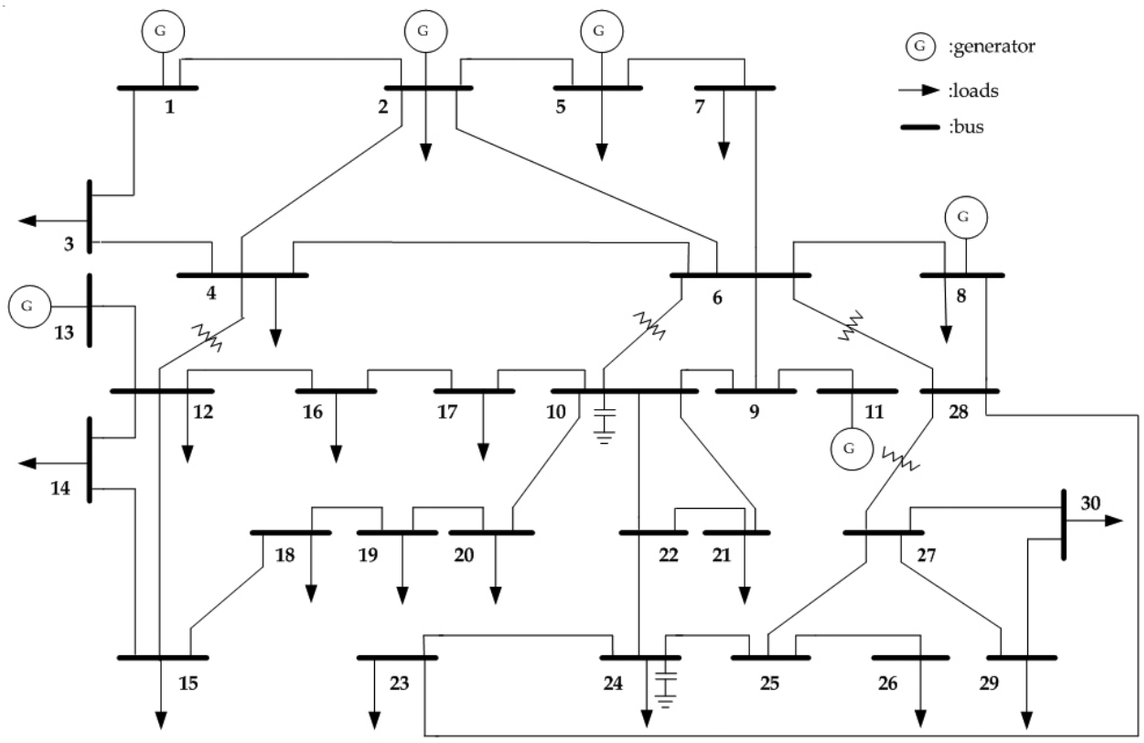

Fig. 5. Measurement configuration of IEEE 30-bus system.

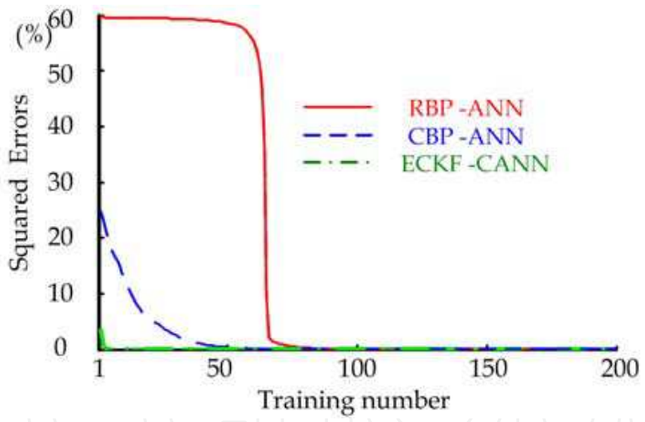

Fig. 6. Comparison of the convergent behavior for three methods.

For the 6-bus test system, the data of 150 time points can be obtained from the original power flow calculation and the first 100 time points are used as the training data of the neural network. For convenient observations, the last 20 time points of the data will be used for bad-data detection. The standard deviations of 0.01 and 0.02 for the bus voltages and the rest of measured data at the last 20 time points will be used for evaluating bad-data detection of ANN during the time duration of the last 20 time points. Similarly, the data measured at the power system of IEEE standard 30-buses will also use the last 20 time points.

Normally, the standard deviation obtained from the measured values at the first 100 time points of the data is used to generate the bad data. However, 20 to 100 times of the standard

deviation was used as the error to add into the measurement in order to generate the bad data [Salehfar & Zhao, 1995]. However, this paper uses 20 times of the standard deviation of the measured values to pollute the measurements. Three of the polluted data will be used for bad-data detection and they are described as below.

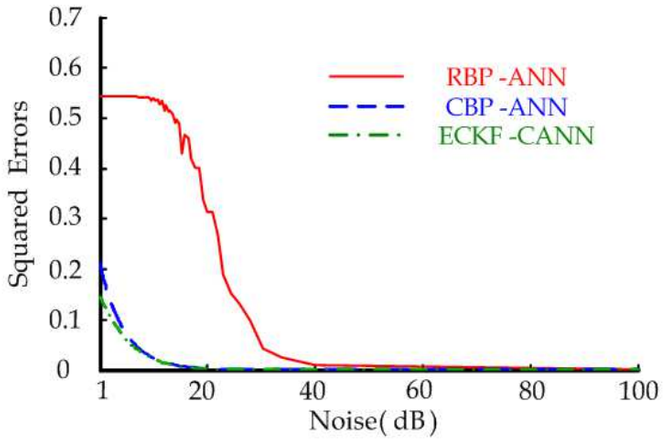

Fig. 7. Comparison of the capacity of noise rejection for three methods.

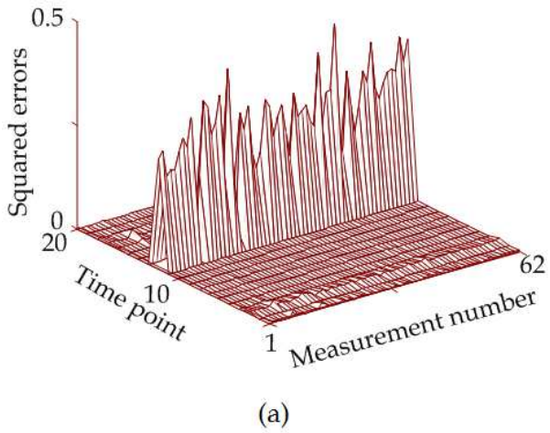

(a)

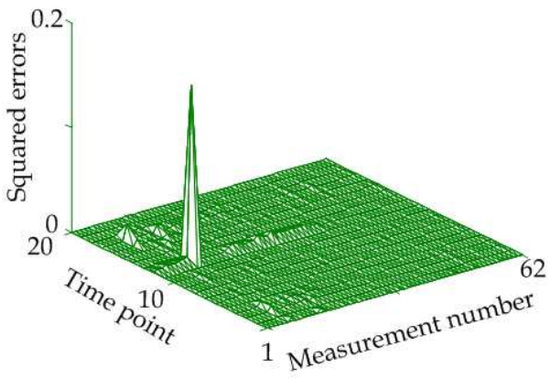

(b)

Fig. 8. Comparison of the squared errors for bad data detection in P_4 using two different methods on a 6-bus system, (a) RBP-ANN, (b) ECKF-CANN.

Case 1: Single bad data

Situation A: 6-bus power system

For the 6-bus system shown in Fig. 4, a measurement at bus 4 (i.e., P_4) numbered as 10 is assumed to have a variation of 20 times standard deviation of the measurement at 12th time point. The squared errors between the measured and estimated values are shown in Fig. 8. As seen from Fig. 8(b), the ECKF-CANN method can effectively detect the bad data of power signals since it only has a pillar spiking out at 12th time point for the measurement number 10. However, the squared errors for each measurement at 12th time point using the RBP-ANN method as seen from Fig. 8(a) are all beyond the threshold value. This means the RBP-ANN method cannot detect the bad data effectively in this case.

Moreover, the estimated measurement at 12th time point using the RBP-ANN and ECKF-CANN methods as estimators are shown in Fig. 9. As seen from Fig. 9(a), the gap between the measured and estimated values at each measurement number is large except the measurement number 10. For example, the estimated and measured values at the measurement number 10 are -0.0464 and -0.144, respectively. Thus, the gap is only 0.0976 with its square error of 0.00953 which is smaller than the gaps of other measurements. Thus, those gaps result in the squared error of some measurements using the RBP-ANN method are beyond the threshold value except the measurement number 10. As seen from Fig. 9(b), the gap between measured and estimated values is large only as the measurement number

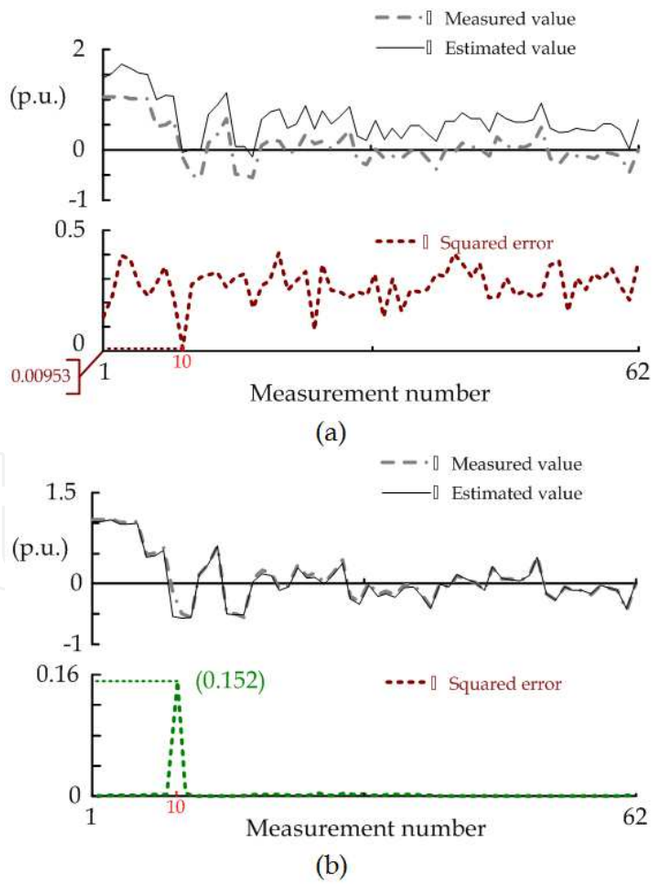

Fig. 9. Estimated results of the estimator at 12th time point using different methods on a 6-bus system, (a) RBP-ANN, (b) ECKF-CANN.

of bad data has occurred. For the measurement number 10, the estimated and measured values are -0.5335 and -0.144, respectively. Thus, the gap will reach 0.3894 with its square error of 0.152. This means the proposed ECKF-CANN method is surely more effective for single bad data detection than the Real-ANN method.

In addition, this chapter uses robust statistics [Mili ,et al,.1996; Pires ,et al,.1999] to obtain robust distances of the measured data for bad data detection under the same condition mentioned above. This method uses a chi-square distribution $(\chi^2_{\nu,0.025})^{1/2}$ with ν degrees of freedom (i.e., ν = n-1, where n is the number of the bus) as a cutoff value to flag the bad data. The detected result of the measurement at 12th time point for the measurement number 10 based on robust statistics is shown in Fig. 10. As can be seen from Fig. 10, the magnitude of the robust distance at the measurement number 10 is about 29.4077 and is greater than the cutoff value 3.582. Thus, the bad data in P_4 can be detected.

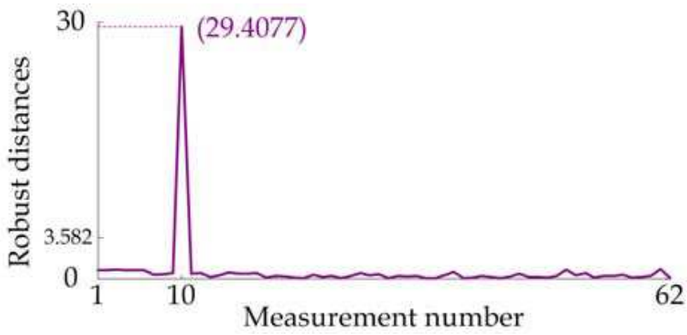

Fig. 10. Estimated results at 12th time point using robust statistics on a 6-bus system.

Situation B: IEEE 30-bus power system

This case assumes the bad data occurs at 12th time point of the P_{14} (i.e., P_{14} is the real power at bus 14) for the measurement number 12. The square errors with only the front 50 measurements obtained by the two methods are shown in Fig. 11. As seen from Fig. 11(b), the squared error reaches 0.406 at 12th time point which is largely greater than the squared errors of other measurements. This means the bad data occurred in the P_{14} can easily be detected. Unlike Fig. 11(b), there are many squared errors obtained by the RBP-ANN method at some measurement numbers as shown in Fig. 11(a). For example, two pillars are spiking out at the measurement number 13 for different time point and the squared error even reaches 0.0304. Nevertheless, the squared error is only 0.00018 at the measurement number 12 at 12th time point. This situation will result a difficulty on detecting the bad data if the threshold value is chosen.

In addition, a bad-data is assumed to occur at the 12th time point of the $P_{1\text{-}3}$ (i.e., $P_{1\text{-}3}$ is the real power of the transmission line flow from bus 1 to bus 3) for the measurement number 10. The threshold used to identify the bad data is predetermined to be 0.0009874 and the standard deviation is computed to be 0.0031423. The test result using the ECKF-CANN method is shown in Fig. 12. As seen from Fig. 12, the squared error is near 0.02 at the 12th time point of the first area and it is greater than the threshold. Thus, it can be used to detect the bad data occurred in the $P_{1\text{-}3}$.

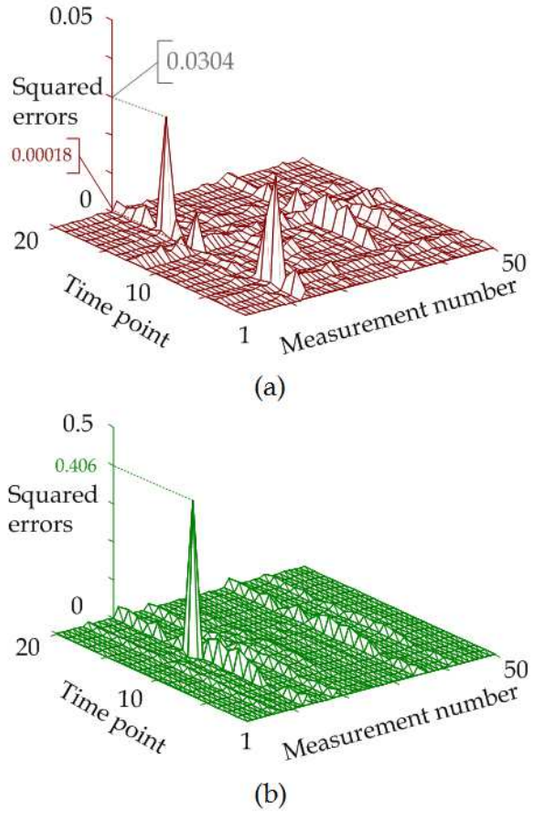

Fig. 11. Squared errors of P_{14} for the IEEE 30-bus system, (a) RBP-ANN, (b) ECKF-CANN.

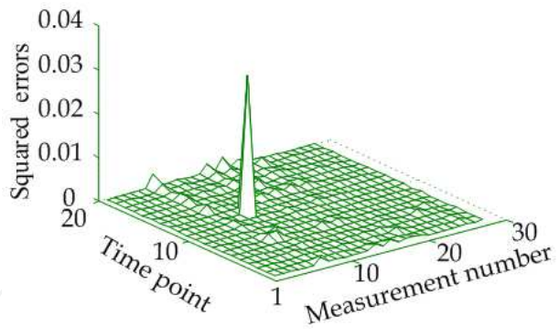

Fig. 12. Squared errors of $P_{1\text{-}3}$ for the 30-bus system using the ECKF-CANN.

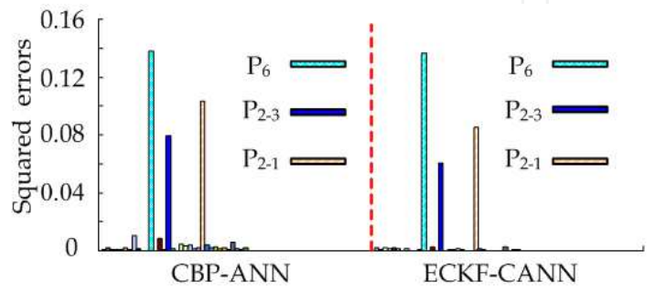

Fig. 13. Comparison of the squared error for the 6-bus system using the CPB-ANN and ECKF-CANN methods.

Case 2: Multiple bad data

Situation A: 6-bus power system

Bad data are assumed to occur in the P_6, $P_{2\text{-}3}$ and $P_{2\text{-}1}$ of the measurement value at the 8th time point. The numbers 12, 22 and 30 are real-type measurements and the numbers 12, 16 and 24 are complex-type measurements. The threshold used to identify the bad data is predetermined to be 0.013938 and the standard deviation is computed to be 0.011806 in the $P_{2\text{-}3}$ measurement value. Comparison of the results using the ECKF-CANN and CBP-ANN methods is shown in Fig. 13. As seen from Fig. 13, the squared errors in the P_6, $P_{2\text{-}3}$ and $P_{2\text{-}1}$ of both methods are all greater than the threshold. However, the results using the CBP-ANN method for detecting other measurements are beyond the threshold. Thus, the detected results were interfered. As seen from the right side in Fig. 13, the squared error of other measurements is smaller than the threshold. This means the ECKF-CANN method is more useful for bad-data detection in power signals.

Similarly, detection of the imaginary part of complex state variable with multiple bad data is tested. The bad data are assumed to occur in the Q_6, $Q_{1\text{-}4}$ and $Q_{4\text{-}1}$ of the measurement value at the 12th time point. As seen from Table 1, the squared errors for detecting Q_6, $Q_{1\text{-}4}$ and $Q_{4\text{-}1}$ are all beyond the threshold value. However, the squared errors in the $Q_{1\text{-}4}$ and $Q_{4\text{-}1}$ using the ECKF-CANN method are greater than those of using the CBP-ANN method. As a result, bad-data detection using the ECKF-CANN method is better than the CBP-ANN method since it has higher squared error.

Methods	Q_6	$Q_{1\text{-}4}$	$Q_{4\text{-}1}$
CBP-ANN	0.99662	0.035799	0.027097
ECKF-CANN	0.60883	0.081422	0.069158

Table 1. The squared error of Q_6, $Q_{1\text{-}4}$ and $Q_{4\text{-}1}$ for the 6-bus system.

Situation B: IEEE 30-bus power system

Bad data are assumed to occur in the measurements of P_2, $P_{5\text{-}7}$ and $P_{7\text{-}6}$ at the 10th time point of the 2nd area. The numbers 6, 19 and 31 are real-type measurements and the numbers 6, 14 and 26 are complex-type measurements. The test results are shown in Fig. 14. As seen from Fig. 14, the RBP-ANN method cannot effectively detect the bad data because its squared errors are all larger than the threshold value of each measurement. However, the CBP-ANN and ECKF-CANN methods can detect the bad data in the P_2, $P_{5\text{-}7}$ and $P_{7\text{-}6}$ at the 10th time point since their squared errors are all beyond the threshold value, as seen from Fig. 14(a) and 14(c).

Case 3: Interacting bad data

Situation A: 6-bus power system

Bad data are assumed to occur in the P_1 and P_4 with excessive errors and in the $P_{1\text{-}2}$ and $P_{3\text{-}2}$ with reverse signs of measurement values at the 10th time point. The numbers 7, 10, 19 and 34 are real-type measurements and the numbers 7, 10, 13 and 28 are complex-type measurements. Comparison of the results using the CBP-ANN and ECKF-CANN methods is summarized in Table 2. As seen from Table 2, the squared error in the $P_{1\text{-}2}$ at the 10th time point using the ECKF-CANN method is greater than that of using the CBP-ANN method. Moreover the square error using the ECKF-CANN method is increased to raise the rate of distinguishing the bad data. This means the ECKF-CANN method is better for detecting the combination of different types of bad data than the CBP-ANN method.

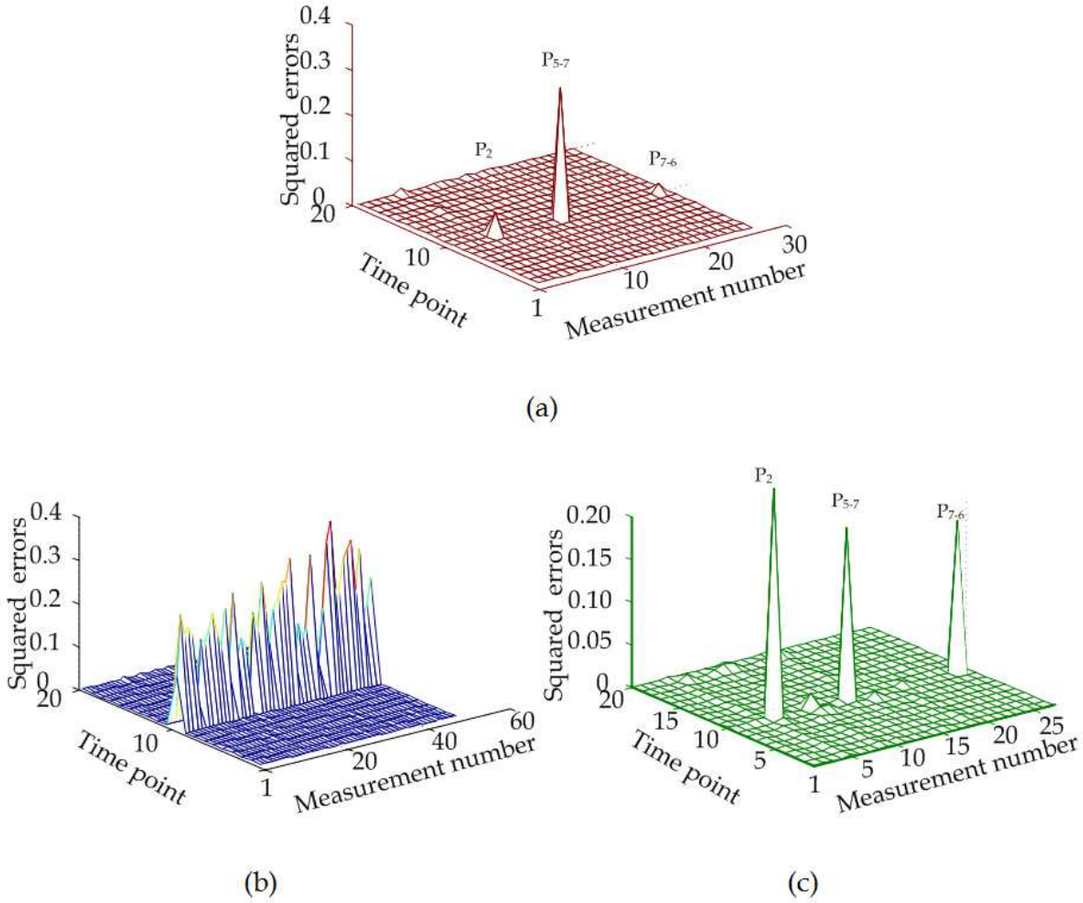

Fig. 14. Comparison of the squared errors for bad-data detection in P_2, $P_{5\text{-}7}$ and $P_{7\text{-}6}$ using three different methods for the 30-bus system, (a) CBP-ANN, (b) RBP-ANN, (c) ECKF-CANN.

Methods	Measured value	Estimated value	Squared error
CBP-ANN	-0.051971	0.056848	0.011842
ECKF-CANN	-0.051971	0.076853	0.016596

Note: The threshold is 0.014329 and the standard deviation is 0.01197.

Table 2. Results for detecting different types of bad data occurring in $P_{1\text{-}2}$.

Situation B: IEEE 30-bus power system

Bad data are assumed to occur in the P_{21} and $P_{9\text{-}10}$ with an excessive error and in the $P_{22\text{-}21}$ and $P_{28\text{-}8}$ with a reverse sign of the measurement values at the 10^{th} time point of the 4^{th} area. The results are shown in Fig. 15. As seen from Fig.15, the ECKF-CANN method can detect the bad data in the measurements of P_{21}, $P_{9\text{-}10}$, $P_{22\text{-}21}$ and $P_{28\text{-}8}$ obviously. But, the squared errors of each measurements of the RBP-ANN at the 10^{th} time point are all beyond the threshold value. Thus, the RBP-ANN cannot judge whether there are bad data polluted in the measurement.

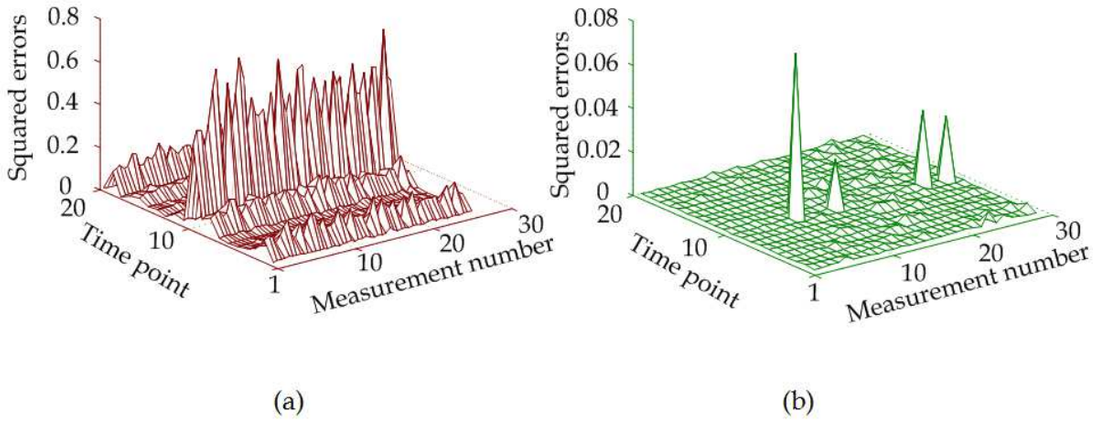

Fig. 15. Comparison of the squared errors for bad-data detection in P_{21}, $P_{9\text{-}10}$, $P_{22\text{-}21}$ and $P_{28\text{-}8}$ using three different methods for the 30-bus system, (a) RBP-ANN, (b) ECKF-CANN.

6. Conclusion

The method with the ECKF learning algorithm based CANN has been developed in this paper to identify the bad-data occurred in a power system. Complex state variables were applied as a link weighting. The proposed method not only can largely reduce node numbers of neurons, but also can search out the suitable and available training variables. Moreover, the ECKF-CANN method converges faster than the traditional algorithms and its capacity of noise rejection is better than the traditional algorithms.

7. References

Teeuwsen, S. P. & Erlich, I. (2006).Neural network based multi-dimensional feature forecasting for bad data detection and feature restoration in power system, *Proceedings of* the 2006 *IEEE General Meeting on Power Engineering Society*, pp. 1-6, ISBN:1-4244-0493-2, June,2006

Zhang, B. M. & Lo, K. L. (1991). A recursive measurement error estimation identification method for bad data analysis in power system state estimation, *IEEE Transactions on power systems*, vol. 6, no. 1, (February 1991)pp. 191-198, ISSN:1558-0679

EI-Keib, A. A.; EI-Sayed, S. M. L. & Brown, H. E. (1989). A model decoupled state estimator with effective bad data identification, *Proceedings of the 1989 IEEE Proceedings Conference on Energy and Information Technologies in the Southeast*, vol. 2, pp. 826-831, Columbia, SC, April 1989

Huang, S. -J. & Lin, J. -M. (2003). A changeable weighting matrix applied for state estimation of electric power, *Proceedings of PEDS the Fifth International Conference on Power Electronics and Drive Systems*, vol. 2, no. 17-20, pp. 873-876, ISBN: 0-7803-7885-7, November 2003

Peterson ,W. L. & Girgis, A. A. (1988). Multiple bad data detection in power system state estimation using linear programming, *Proceedings of the Twentieth Southeastern Symposium on System Theory*, pp. 405-409, ISBN: 0-8186-0847-1, Charlotte, NC, March 1988

Abur, Ali (1990). A bad data identification method for linear programming state estimation, *IEEE Transactions on Power Systems*, vol. 5, no. 3, (August 1990) pp. 894-901, , ISSN: 1558-0679

Zhang, B. M. ;Wang, S. Y. & Xiang, N. D. (1992). A linear recursive bad data identification method with real-time application to power system state estimation, *IEEE Transactions on Power Systems*, vol. 7, no. 3, (August 1992)pp. 1378-1385, ISSN: 1558-0679

Huang, S. -J. & Lin, J. -M. (2002). Enhancement of power system data debugging using GSA-based data mining technique, *IEEE Transactions on power systems*, vol. 17, no. 4, (November 2002)pp. 1022-1029, ISSN: 1558-0679

Huang S. -J. & Lin, J. -M. (2004). Enhancement of anomalous data mining in power system predicting-aided state estimation, *IEEE Transactions on power systems*, vol. 19, no. 1, , (February 2004) pp. 610-619, ISSN: 1558-0679

Souza, J. C. S.; Leite da Silva A. M. & Alves da Silva, A. P. (1998). Online topology determination and bad data suppression in power system operation using artificial neural networks," *IEEE Transactions on Power Systems*, vol. 13, no. 3, (August 1998) pp. 796-803, ISSN: 1558-0679

Alves da Silva ,A. P.; Quintana , V. H. & Pang, G. K. H. (1992). Associative memory models for data processing, *International Journal of Electrical Power & Energy Systems*, vol. 14, no. 1, (February 1992) pp. 23-32, SSDI: 0142-0615

Deergha Rao, K. (1996). Narrowband direction finding using complex EKF trained multilayered neural Networks, *Proceedings of the 1996 IEEE 3rd International Conference on Signal Processing,* vol. 2, pp. 1377-1380, ISBN: 0-7803-2912-0, Beijing, October 1996

Deergha Rao K.; Swamy,M. N. S. & Plotkin, E. I. (2000). Complex EKF neural network for adaptive equalization, *Proceedings of the 2000 IEEE International Symposium on Circuits and Systems*, vol. 2, pp. 349-352, ISBN: 0-7803-5482-6, Geneva, May 2000

Taehwan Kim & Adali, T. (2000). Fully complex backpropagation for constant envelope signal processing, *Proceedings of the 2000 IEEE Signal Processing Society Workshop*, vol.1, pp. 231-240, ISBN: 0-7803-6278-0, Sydney NSW, December 2000

Salehfar, H. & Zhao, R. (1995). A neural network preestimation filter for bad-data detection and identification in power system state estimation, *Electric Power System Research*, vol. 34, no. 2, (February 1995) pp.127-134, SSDI: 0378-7796

Mili, L.; Cheniae, M. G.; Vichare, N. S. & Rousseeuw, P. J. (1996). Robust state estimation based on projections statistics, *IEEE Transactions on Power Systems*, vol. 11, no. 2, (May 1996)pp. 1118-1127, ISSN: 1558-0679

Pires, R. C.; Costa, A. J. A. S. & Mili, L.(1999).Iteratively reweighted least-squares state estimation through givens rotations, *IEEE Transactions on Power Systems*, vol. 14, no. 4, (November 1999)pp. 1499-1507, ISSN: 1558-0679

Kalman Filter

Edited by Vedran Kordic

ISBN 978-953-307-094-0
Hard cover, 390 pages
Publisher InTech
Published online 01, May, 2010
Published in print edition May, 2010

The Kalman filter has been successfully employed in diverse areas of study over the last 50 years and the chapters in this book review its recent applications. The editors hope the selected works will be useful to readers, contributing to future developments and improvements of this filtering technique. The aim of this book is to provide an overview of recent developments in Kalman filter theory and their applications in engineering and science. The book is divided into 20 chapters corresponding to recent advances in the filed.

InTech Europe
University Campus STeP Ri
Slavka Krautzeka 83/A
51000 Rijeka, Croatia
Phone: +385 (51) 770 447
Fax: +385 (51) 686 166
www.intechopen.com

InTech China
Unit 405, Office Block, Hotel Equatorial Shanghai
No.65, Yan An Road (West), Shanghai, 200040, China
中国上海市延安西路65号上海国际贵都大饭店办公楼405单元
Phone: +86-21-62489820
Fax: +86-21-62489821

IntechOpen